

# Alarm Deadband Design Based on Maximum Amplitude Deviations and Bayesian Estimation

Jiandong Wang<sup>ID</sup>, Senior Member, IEEE, Shouchen Sun<sup>ID</sup>, Zhen Wang<sup>ID</sup>, Xuan Zhou, and Poku Gyasi<sup>ID</sup>

**Abstract**—Alarm deadbands are commonly used in modern computerized monitoring systems to avoid false alarms. A new method is proposed to design an alarm deadband, to achieve a desired percentage of removed false alarms with respect to the counterparts without using an alarm deadband. An optimal value of the deadband width is determined based on the cumulative probability of maximum amplitude deviations between an alarm threshold and values of a process variable in the alarm state. The Bayesian estimation approach is used to evaluate whether the estimated cumulative probability is reliable and whether the designed deadband width is trustworthy. Existing methods are either limited to independently and identically distributed (IID) process variables or require complicated techniques of Kalman filters or particle filters for non-IID ones. By contrast, the proposed method is simple for implementation and has no discriminations to IID and non-IID process variables. Numerical and industrial examples are provided to support the proposed method.

**Index Terms**—Alarm deadbands, alarm systems, Bayesian estimation, false alarms.

## I. INTRODUCTION

IN MODERN industrial plants, a larger amount of process variables are monitored in a real-time manner [1], [2]. If an abnormal condition occurs, some process variables overpass alarm thresholds so that alarm events are generated automatically with audible sounds, popping-up messages, or flashing lights, to attract the attention of industrial plant operators. As an integrated part of automatic monitoring systems, alarm generators play very important roles in the safety and efficiency of modern industrial plants [3], [4], [5].

The alarm overloading problem refers to a phenomenon that there are too many alarm events to be handled by industrial plant operators [6]. For instance, some industrial surveys indicated that average numbers of alarm events per day could reach up to 1200, 1500, and 2000, respectively, for oil and gas, petrochemical, and power plants [4]. False alarms are major culprits to the alarm overloading problem; they are presented due to some causes such as the presence of noises, even though process variables being monitored are actually under normal operating conditions and abnormalities are absent [7].

Manuscript received 22 November 2022; accepted 22 January 2023. Date of publication 3 February 2023; date of current version 22 June 2023. This work was supported in part by the National Natural Science Foundation of China under Grant 61433001. Recommended by Associate Editor L. Imsland. (Corresponding author: Jiandong Wang.)

The authors are with the College of Electrical Engineering and Automation, Shandong University of Science and Technology, Qingdao, Shandong 266590, China (e-mail: jiandong@sdust.edu.cn; ssc980828@163.com; wzz4585@163.com; xuanzhou178@163.com; pokugyasi4@gmail.com).

Color versions of one or more figures in this article are available at <https://doi.org/10.1109/TCST.2023.3240020>.

Digital Object Identifier 10.1109/TCST.2023.3240020

Alarm deadbands and delay timers are embedded functions in modern computerized monitoring systems such as distributed control systems to avoid false alarms [1], [2], [3], [4], [5]. Unlike a common way of raising an alarm event when a process variable  $x(t)$  overpasses an alarm threshold  $x_{th}$ , an alarm deadband raises an alarm event when  $x(t)$  overpasses  $x_{th} + \delta_d$  for a high alarm or  $x_{th} - \delta_d$  for a low alarm and clears the alarm event when  $x(t)$  goes back to  $x_{th}$ . A delay timer announces (clears) an alarm event when consecutive samples of  $x(t)$  overpass (go back to)  $x_{th}$ , instead of one single sample of  $x(t)$  [8], [9]. The application scenarios are different: alarm deadbands are suitable to deal with false alarms when  $x(t)$  deviates not too far away from  $x_{th}$  for a long time, while delay timers are good for false alarms when  $x(t)$  traverses  $x_{th}$  quickly.

The deadband width  $\delta_d$  is the parameter to be designed for an alarm deadband. Bransby and Jenkinson [3] recommended default values of  $\delta_d$  in the percentage of operating ranges of  $x(t)$ , such as 5% for flow and level variables, 2% for pressure variables, and 1% for temperature variables. These default values were later adopted by the International Society of Automation (ISA) standard [1] and the Engineering Equipment and Materials Users' Association (EEMUA) guideline [2]. Rothenberg [4] suggested  $\delta_d$  to be about 20% larger than normal noise values, which required a difficult task of separating noises from measurements. Hugo [11] represented process variables in an autoregressive-integrated moving-average model, based on which a deadband width was determined via the Kalman filter. Izadi et al. [12] designed alarm deadbands by balancing false and missed alarm rates, whose analytic expressions were derived from a Markov model to describe transitions of alarm and nonalarm states for independently and identically distributed (IID) process variables. Adnan et al. [13] and Naghoosi et al. [14] further exploited the Markov model to calculate expected detection delays between occurrences of alarm events and abnormalities for alarm deadbands under the assumption of IID process variables. Afzal et al. [15] derived analytical expressions of the false alarm rate (FAR), missed alarm rate, and expected detection delay for time deadbands based on Markov models. Han et al. [16] set up adaptive deadband widths based on standard deviations of Gaussian-distributed process variables in short fixed time windows. Tulsyan and Gopaluni [17] considered a type of process variables being described by a stochastic nonlinear time-series model and applied particle filters to obtain required joint probability functions of process variables for designing alarm deadbands. Wang et al. [18] obtained an optimal deadband width to minimize a weighted summation of FARs and pseudo-delay factors being normalized

with respect to their acceptable maximum values. Aslansefat et al. [19] evaluated some performance indices of adaptive alarm thresholds and adaptive deadbands for IID process variables. Nunes et al. [20] designed an optimal deadband width by minimizing a quadratic sum of the FAR and missed alarm rate based on their expressions given in [12]. Asaadi et al. [21] calculated the FAR, missed alarm rate, and expected detection delay based on finite mixture models to describe intermittent faults. Most of the above methods are either limited to IID process variables or require complicated techniques of Kalman filters or particle filters for non-IID ones.

The brief proposes a new method to design alarm deadbands for removing false alarms, by taking a different viewpoint from most of the existing methods in the literature. A random variable is introduced as the maximum amplitude deviation between the alarm threshold and values of a process variable running into the alarm state. It is observed that by using an alarm deadband with the width  $\delta_d$ , all false alarms being associated with maximum amplitude deviations smaller than  $\delta_d$  will be removed. An optimal value of  $\delta_d$  is determined from a cumulative probability of the maximum amplitude deviation to achieve a desired percentage of removed false alarms with respect to the counterparts without using an alarm deadband. The Bayesian estimation approach is used to estimate the cumulative probability together with its confidence interval and to evaluate whether the designed deadband width is trustworthy.

The proposed method essentially requires a cumulative probability of the maximum amplitude deviation, so that it is simple for implementation in practice and has no discriminations to IID and non-IID process variables. On the contrary, some existing methods are based on the probability distribution functions of process variables that have to be assumed IID; for non-IID process variables, existing methods need to build time-series models and involve complicated techniques of Kalman filters and particle filters.

The rest of this brief is organized as follows. Section II describes the problem to be solved. Section III presents the proposed method. Section IV provides numerical and industrial examples as illustrations. Section V concludes the brief.

## II. PROBLEM FORMULATION

This section describes the problem of designing alarm deadbands to remove false alarms. An alarm event is usually raised when a process variable  $x(t)$  overpasses an alarm threshold  $x_{th}$ , that is,

$$x_a(t) = \begin{cases} 1, & \text{if } x(t) \geq (\leq) x_{th} \\ 0, & \text{if } x(t) < (>) x_{th}. \end{cases} \quad (1)$$

The value of 1 (0) is assigned to the alarm variable  $x_a(t)$  for the alarm (nonalarm) state. The constant  $x_{th}$  is a high (low) alarm threshold. The sampling index  $t$  takes a positive integer value and is associated with a sampling period  $h$  (e.g.,  $h = 0.5$  s). Ideally,  $x_a(t)$  takes the value of 1 if and only if  $x(t)$  runs into an abnormal condition, so that each alarm event stands for the presence of an abnormal condition. However, many alarm variables are suffering from a large

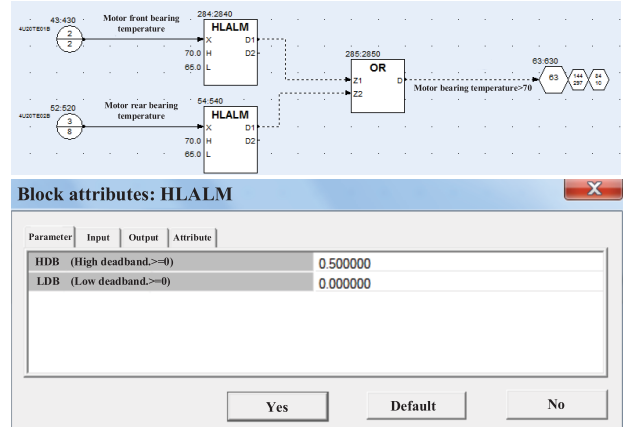


Fig. 1. Embedded alarm deadband function in distributed control systems.

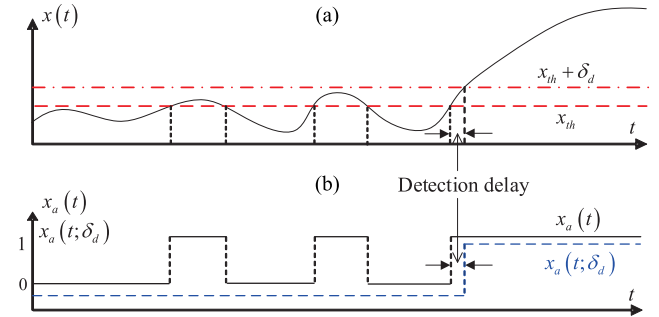


Fig. 2. (a)  $x(t)$  (black solid), the high-alarm threshold  $x_{th}$  (red dash) and  $x_{th} + \delta_d$  (red dot-dash). (b)  $x_a(t)$  (black solid),  $x_a(t; \delta_d)$  (blue dash, shifted downward for 0.1).

amount of false alarms that are caused by noises, instead of abnormal conditions.

Alarm deadbands are powerful tools that are frequently used in practice to remove false alarms [4]. For a high alarm threshold, an alarm deadband with the width  $\delta_d$  raises an alarm event if  $x(t)$  is larger than or equal to  $x_{th} + \delta_d$  and clears an alarm event if  $x(t)$  is smaller than  $x_{th}$ , that is,

$$x_a(t; \delta_d) = \begin{cases} 1, & \text{if } x(t) \geq x_{th} + \delta_d \\ 0, & \text{if } x(t) < x_{th} \\ x_a(t - 1; \delta_d), & \text{otherwise.} \end{cases} \quad (2)$$

Thus, two thresholds are used to raise and clear alarm events. Analogously, an alarm deadband is defined for a low alarm threshold

$$x_a(t; \delta_d) = \begin{cases} 1, & \text{if } x(t) \leq x_{th} - \delta_d \\ 0, & \text{if } x(t) > x_{th} \\ x_a(t - 1; \delta_d), & \text{otherwise.} \end{cases} \quad (3)$$

The alarm deadband is commonly implemented as an embedded function in distributed control systems, for example, the high low alarm (HLALM) function depicted in Fig. 1. The parameters high deadband (HDB) and low deadband (LDB) in the function are the counterparts of  $\delta_d$  in (2) and (3), respectively. In the sequel, the alarm deadband for a high alarm threshold is considered without the loss of generality.

The functionality of an alarm deadband is illustrated in Fig. 2. Some samples of  $x(t)$  are larger than a high alarm

threshold  $x_{\text{th}}$ , but are smaller than  $x_{\text{th}} + \delta_d$ . As a result, some false alarms are present in  $x_a(t)$ , but are absent in  $x_a(t; \delta_d)$ . Clearly, more false alarms can be removed for a larger value of  $\delta_d$ ; however, the price is the increment of a detection delay between the time instant of  $x_a(t)$  running to the alarm state and that of  $x_a(t; \delta_d)$  switching from “0” to “1,” both due to the same abnormal condition. Hence,  $\delta_d$  should be chosen to make a good balance between the detection delay and the number of false alarms to be removed. Doing so requires historical samples of  $x(t)$  in abnormal conditions, because the time instants of  $x_a(t)$  and  $x_a(t; \delta_d)$  running into alarm states are dependent on when the samples of  $x(t)$  in abnormal conditions go beyond  $x_{\text{th}}$  and  $x_{\text{th}} + \delta_d$ , respectively. However, historical samples in abnormal conditions are hardly available, because a majority of process variables from an industrial plant stay at normal conditions for most of the time instances and run into abnormal conditions occasionally. Hence, this brief designs alarm deadbands solely based on historical samples in normal conditions. Adnan et al. [13] presented the relationship between the deadband width and two performance indices of the FAR and detection delay: when the deadband width increases, the FAR decreases and the detection delay increases accordingly. Therefore, the detection delay can be implicitly considered by selecting a proper value of the deadband width to control the number of false alarms to be removed, instead of removing all false alarms.

The objective of this brief is to design an optimal value of the deadband width  $\delta_d$  based on historical samples of  $\{x(t)\}_{t=1}^N$  in normal conditions. The optimality lies in choosing  $\delta_d$  such that the percentage of false alarms in  $x_a(t; \delta_d)$  with respect to the counterparts in  $x_a(t)$  is closest to a desired value.

### III. PROPOSED METHOD

This section proposes a method to design the deadband width based on historical samples in normal conditions.

First, some basic concepts are introduced. An alarm event is also known as an alarm occurrence that  $x_a(t)$  switches from the nonalarm state “0” to the alarm state “1,” that is,

$$x_{a,o}(t) = \begin{cases} 1, & \text{if } x_a(t-1) = 0 \text{ \& } x_a(t) = 1 \\ 0, & \text{otherwise.} \end{cases} \quad (4)$$

Analogously, an alarm clearance is

$$x_{a,c}(t) = \begin{cases} 1, & \text{if } x_a(t-1) = 1 \text{ \& } x_a(t) = 0 \\ 0, & \text{otherwise.} \end{cases} \quad (5)$$

In general, alarm occurrences and clearances are presented in pairs. The  $k$ th paired alarm occurrence and clearance are respectively associated with the sampling indices  $t_o(k)$  and  $t_c(k)$  such that

$$x_{a,o}(t_o(k)) = 1, \quad x_{a,c}(t_c(k)) = 1 \\ \sum_{t=t_o(k)}^{t_c(k)} x_a(t) = t_c(k) - t_o(k), \quad \text{for } t_c(k) > t_o(k). \quad (6)$$

The  $k$ th maximum amplitude deviation is defined as the maximum value of deviations between  $x_{\text{th}}$  and  $\{x(t)\}_{t=t_o(k)}^{t_c(k)}$

$$\delta(k) = \max \left( \left| \{x(t) - x_{\text{th}}\}_{t=t_o(k)}^{t_c(k)-1} \right| \right). \quad (7)$$

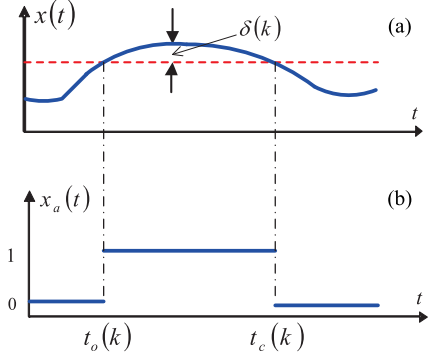


Fig. 3. (a)  $x(t)$  (blue solid) and the high-alarm threshold  $x_{\text{th}}$  (red dash). (b)  $x_a(t)$  (blue solid).

Fig. 3 illustrates the alarm occurrence, alarm clearance, and maximum amplitude deviation. It is ready to obtain a sample set  $\{\delta(k)\}_{k=1}^K$  from  $\{x(t)\}_{t=1}^N$ . A comparison between (2) and (7) says that if  $\delta(k)$  is less than the deadband width  $\delta_d$ , then the  $k$ th alarm occurrence in  $x_a(t)$  will not appear in  $x_a(t; \delta_d)$ . Hence,  $\delta_d$  can be designed based on certain information of  $\{\delta(k)\}_{k=1}^K$ .

Second, an optimization function is formulated. If  $\{x(t)\}_{t=1}^N$  is in the normal condition, the number of false alarms is

$$F(\{x_a(t)\}_{t=1}^N) = \sum_{t=1}^N x_{a,o}(t). \quad (8)$$

The effectiveness of an alarm deadband is measured by the ratio of the number of false alarms in  $\{x_a(t)\}_{t=1}^N$  with respect to the counterpart in  $\{x_a(t; \delta_d)\}_{t=1}^N$ , that is,

$$\eta(\delta_d) = \frac{F(\{x_a(t; \delta_d)\}_{t=1}^N)}{F(\{x_a(t)\}_{t=1}^N)}. \quad (9)$$

The ratio  $\eta(\delta_d)$  is in the range  $[0, 1]$ . If  $\eta(\delta_d)$  is closer to zero, then more false alarms in  $x_a(t)$  are removed. As discussed in Section II,  $\delta_d$  cannot be too large to avoid an excessive value of the abnormality detection delay. An optimal value of  $\delta_d$  is chosen as the one to make  $\eta(\delta_d)$  in (9) closest to a user-selected desired value  $\eta_0$ , that is,

$$\delta_{\text{opt}} = \min\{\delta_{\text{max}}, \arg \min_{\delta_d} |\eta(\delta_d) - \eta_0|\}. \quad (10)$$

Here,  $\eta_0$  has a similar physical meaning as the probability of type-I errors in statistics [22], [23], because false alarms appear in normal conditions and belong to type-I errors. The probability of type-I errors is usually chosen as 1% or 5% [22], [23]. In this brief, a default value of  $\eta_0$  is taken as 5%.

The parameter  $\delta_{\text{max}}$  in (10) is an upper bound of deadband widths, to avoid missing correct alarms. If historical samples of  $x(t)$  in abnormal conditions are available, they can be exploited to design a proper value of  $\delta_{\text{max}}$ . However, those samples are hardly available as discussed earlier in Section II. Based on historical samples  $\{x(t)\}_{t=1}^N$  in normal conditions,  $\delta_{\text{max}}$  is designed in two steps as given in our previous work [18]: 1)  $x_{\text{th}}$  is reset as the mean value of  $\{x(t)\}_{t=1}^N$ , and  $\{\delta(k)\}_{k=1}^K$  in (7) is recalculated by using the reset value of  $x_{\text{th}}$ ; and 2)  $\{\delta(k)\}_{k=1}^K$  is sorted in the ascending order as

$\{\delta'(k)\}_{k=1}^K$ , whose 95th percentile is taken as  $\delta_{\max}$ , that is,

$$\delta_{\max} = \delta'(\lceil 0.95 \cdot K \rceil). \quad (11)$$

Here,  $\lceil \cdot \rceil$  is the ceil function taking the smallest integer larger than the operand.

The maximum amplitude deviation  $\delta(k)$  in (7) can be regarded as a realization of a continuous random variable  $\Delta$  with the probability density function (pdf)  $f_\Delta(\delta)$ . It is reasonable to assume that alarm occurrences are mutually independent, so that  $\eta(\delta_d)$  in (9) is equivalent to the area covered by  $f_\Delta(\delta)$  above the value  $\delta_d$ , that is,

$$\eta(\delta_d) = \int_{\delta_d}^{+\infty} f_\Delta(\delta) d\delta. \quad (12)$$

Thus, determining  $\delta_{\text{opt}}$  in (10) is equivalent to calculating the cumulative probability in (12). By introducing a symbol

$$\Theta(\delta_d) := \int_{\delta_d}^{+\infty} f_\Delta(\delta) d\delta \quad (13)$$

$\delta_{\text{opt}}$  in (10) becomes

$$\delta_{\text{opt}} = \min\{\delta_{\max}, \arg \min_{\delta_d} |\Theta(\delta_d) - \eta_0|\}. \quad (14)$$

The main concern is how to obtain a reliable estimate of  $\Theta(\delta_d)$ . Note that the probability  $\Theta(\delta_d)$  is required here; such a requirement is much less demanding than the estimation of the pdf  $f_\Delta(\delta)$ . Note that the pdf of  $x(t)$  is not required so that the IID or non-IID assumption of  $x(t)$  is irrelevant.

Third, a reliable estimate of the cumulative probability  $\Theta(\delta_d)$  in (13) is obtained by the Bayesian estimation approach. The probability that  $\delta(k)$  falls inside an interval  $[\delta_0, +\infty]$  for a certain value  $\delta_0$  is approximately equal to

$$\Theta(\delta_0) = \frac{c(\delta_0)}{K} \quad (15)$$

where  $c(\delta_0)$  is the number of samples in  $\{\delta(k)\}_{k=1}^K$  to satisfy  $\delta(k) \geq \delta_0$ . For the Bayesian estimation approach [24],  $\Theta(\delta_0)$  is not treated as an unknown constant in the range  $(0, 1)$ , but is regarded as a continuous random variable  $\Theta(\delta_0)$  taking  $\theta(\delta_0)$  as a realization. If no extra information is available, the prior pdf of  $\Theta(\delta_0)$  is usually taken as a continuous uniform distribution

$$f_{\Theta(\delta_0)}(\theta(\delta_0)) = \begin{cases} 1, & 0 < \theta(\delta_0) < 1 \\ 0, & \text{otherwise.} \end{cases} \quad (16)$$

Let us take the number of elements in  $\{\delta(k)\}_{k=1}^K$  falling inside  $[\delta_0, +\infty]$  as a realization  $c(\delta_0)$  of a discrete random variable  $C(\delta_0)$ . Since maximum amplitude deviations are mutually independent,  $C(\delta_0)$  takes the binomial distribution with the probability of success as  $\Theta(\delta_0)$  among  $K$  independent trials with two outcomes of success and failure [24]. The conditional pdf of  $C(\delta_0)$  based on  $\Theta(\delta_0)$  is

$$f_{C(\delta_0)|\Theta(\delta_0)}(c(\delta_0)|\theta(\delta_0)) = \frac{c(\delta_0)!}{c(\delta_0)!(K - c(\delta_0))!} \cdot (\theta(\delta_0))^{c(\delta_0)} \cdot (1 - \theta(\delta_0))^{K - c(\delta_0)}. \quad (17)$$

The Bayesian formula yields the posterior pdf of  $\Theta(\delta_0)$  based on the realization  $c(\delta_0)$  of  $C(\delta_0)$

$$f_{\Theta(\delta_0)|C(\delta_0)}(\theta(\delta_0)|c(\delta_0)) = \frac{f_{C(\delta_0), \Theta(\delta_0)}(c(\delta_0), \theta(\delta_0))}{f_{C(\delta_0)}(c(\delta_0))} \quad (18)$$

where the joint pdf of  $C(\delta_0)$  and  $\Theta(\delta_0)$  is

$$f_{C(\delta_0), \Theta(\delta_0)}(c(\delta_0), \theta(\delta_0)) = f_{C(\delta_0)|\Theta(\delta_0)}(c(\delta_0)|\theta(\delta_0)) \cdot f_{\Theta(\delta_0)}(\theta(\delta_0)) \quad (19)$$

and the marginal pdf of  $C(\delta_0)$  is

$$f_{C(\delta_0)}(c(\delta_0)) = \int f_{C(\delta_0), \Theta(\delta_0)}(c(\delta_0), \theta(\delta_0)) d\theta(\delta_0). \quad (20)$$

The Bayesian estimate of  $\theta(\delta_0)$  is often taken as the conditional mean

$$\hat{\theta}(\delta_0) = \int \theta(\delta_0) \cdot f_{\Theta(\delta_0)|C(\delta_0)}(\theta(\delta_0)|c(\delta_0)) d\theta(\delta_0). \quad (21)$$

It is ready to obtain the  $(1 - \alpha)$  confidence interval of  $\theta(\delta_0)$  from (18) as the narrowest interval  $[\hat{\theta}_-(\delta_0), \hat{\theta}_+(\delta_0)]$  satisfying the equality

$$\int_{\hat{\theta}_-(\delta_0)}^{\hat{\theta}_+(\delta_0)} f_{\Theta(\delta_0)|C(\delta_0)}(\theta(\delta_0)|c(\delta_0)) d\theta(\delta_0) = 1 - \alpha. \quad (22)$$

A default value  $\alpha = 0.05$  is used for the 95% confidence level. If the difference between  $\hat{\theta}(\delta_0)$  and  $\hat{\theta}_-(\delta_0)$  and that between  $\hat{\theta}(\delta_0)$  and  $\hat{\theta}_+(\delta_0)$  are small with respect to  $\hat{\theta}(\delta_0)$ , for example,

$$r(\hat{\theta}(\delta_0)) := \frac{\hat{\theta}(\delta_0)}{\max(\hat{\theta}(\delta_0) - \hat{\theta}_-(\delta_0), \hat{\theta}_+(\delta_0) - \hat{\theta}(\delta_0))} \geq \beta \quad (23)$$

then  $\hat{\theta}(\delta_0)$  is regarded as a reliable estimate of  $\Theta(\delta_0)$  in (15). As the Bayesian estimation approach yields a consistent estimate [24], the confidence interval  $[\hat{\theta}_-(\delta_0), \hat{\theta}_+(\delta_0)]$  in (22) will be narrower when the sample size  $K$  of  $\{\delta(k)\}_{k=1}^K$  is larger. Hence, it is expected that  $r(\hat{\theta}(\delta_0))$  in (23) gets larger as  $K$  increases. The parameter  $\beta$  is a threshold of  $r(\hat{\theta}(\delta_0))$  as the ratio of the estimate  $\hat{\theta}(\delta_0)$  to its estimation uncertainty. A sensitivity analysis of  $\beta$  given later in Example 1 at Section IV shows that if  $\beta$  is not less than 1, then the designed deadband width is no longer sensitive to  $\beta$ . Hence, a default value  $\beta = 1$  is used to say that  $\hat{\theta}(\delta_0)$  should be equal to or larger than its estimation uncertainty.

In summary, the alarm deadband is designed based on historical samples  $\{x(t)\}_{t=1}^N$  in the normal condition as follows.

- 1) Step 1: Samples of the maximum amplitude deviation  $\delta(k)$  in (7) are collected from  $\{x(t)\}_{t=1}^N$  as  $\{\delta(k)\}_{k=1}^K$ , and  $\delta_{\max}$  in (11) is obtained.
- 2) Step 2: The Bayesian estimate  $\hat{\theta}(\delta_0)$  in (21) and its confidence interval  $[\hat{\theta}_-(\delta_0), \hat{\theta}_+(\delta_0)]$  in (22) are calculated on the basis of  $\{\delta(k)\}_{k=1}^K$ . If  $r(\hat{\theta}(\delta_0))$  in (23) is large enough, then proceed to the next step; otherwise, the above two steps are repeated for more samples of the maximum amplitude deviation.
- 3) Step 3: The optimal deadband width is  $\delta_{\text{opt}} = \delta_0$  as the solution to the problem in (10) or equivalently that in (14).

The pseudo-code of above steps is given in Algorithm 1. MATLAB programs for implementing the steps are accessible

**Algorithm 1** Design of the Optimal Deadband Width  $\delta_{opt}$ 

**Input:** The process variable  $x(t)$ , alarm threshold  $x_{th}$ , user-selected desired value  $\eta_0$   
**Output:** The optimal deadband width  $\delta_{opt}$

- 1: Begin
- 2: **repeat**
- 3:     Obtain samples of the maximum amplitude deviation  $\delta(k)$  in Eq. (7);
- 4:     Compute the upper bound  $\delta_{max}$  of deadband widths as the one in Eq. (11);
- 5:     Calculate the Bayesian estimate of  $\theta(\delta_0)$  in Eq. (21);
- 6: **until**  $r(\hat{\theta}(\delta_0)) \geq \beta$  in Eq. (23);
- return The optimal deadband width  $\delta_{opt}$  in Eq. (10)

at <https://ieeexplore.ieee.org/document/9333333>. The integral to calculate  $\hat{\theta}(\delta_0)$  in (21) is implemented as a numerical integration by discretizing  $\theta(\delta_0)$  and  $\delta_0$ . In particular,  $\theta(\delta_0)$  is discretized in the range  $(0, 1)$  by a small step size, for example, 0.001, since  $\theta(\delta_0)$  represents a possible value of the probability of false alarms;  $\delta_0$  is discretized in the range  $(0, \delta_{max})$  by a proper step size, for example,  $0.01 \cdot x_{th}$ , since  $\delta_0$  stands for a possible value of the deadband width. For Step 2, if there are not enough samples of the maximum amplitude deviation, the proposed method can still proceed to Step 3; however, the optimal deadband width designed in Step 3 may not be reliable to achieve the desired value  $\eta_0$  for new samples of  $x(t)$ .

Alarm deadbands are very effective for process variables that are lingering around the alarm threshold with small amplitude deviations possibly for several consecutive samples. As depicted in Fig. 2, these kinds of process variables are not IID. Hence, most of the design methods based on the IID assumption of process variables are suffering from such an invalid assumption. For non-IID process variables, Hugo [11] or Tulsyan and Gopaluni [17] built time-series models to describe  $x(t)$  and exploited Kalman filters or particle filters to design  $\delta_d$ ; however, it is a well-known fact that building time-series models is not an easy task in general. By contrast, the proposed method requires a cumulative probability of the maximum amplitude deviation  $\delta(k)$ , instead of the pdfs or time-series models of  $x(t)$ , so that the proposed method is easy to implement and has no discriminations to IID and non-IID process variables.

## IV. EXAMPLES

This section presents numerical and industrial examples to illustrate the proposed method.

*Example 1:* This numerical example validates the estimated cumulative probability of maximum amplitude deviations and compares the proposed method with existing ones based on the IID assumption of process variables. Consider a moving average process

$$x(t) = \frac{1}{4} \sum_{i=1}^4 e(t-i) \quad (24)$$

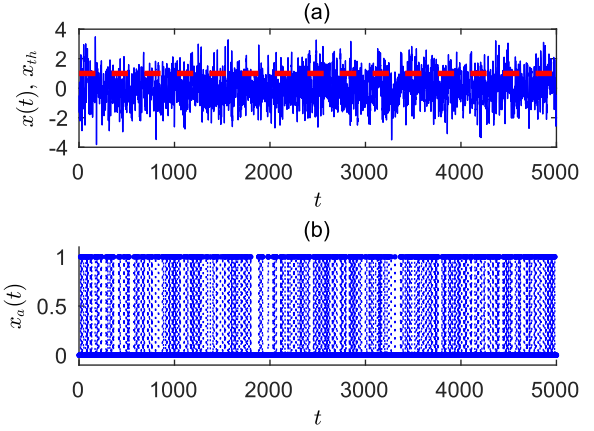


Fig. 4. (a)  $x(t)$  (blue solid) and a high-alarm threshold  $x_{th}$  (red dash). (b)  $x_a(t)$  in Example 1.

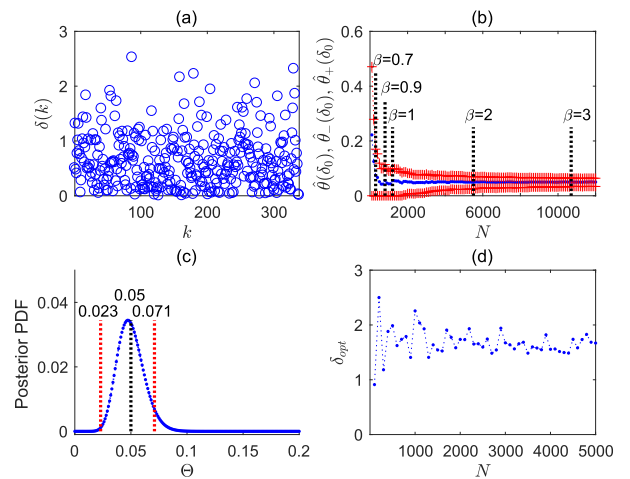


Fig. 5. (a) Maximum amplitude deviations  $\{\delta(k)\}_{k=1}^{K=338}$  for  $N = 5000$ . (b) Estimated cumulative probability  $\hat{\theta}(\delta_0)$  (blue dot) and its confidence interval  $[\hat{\theta}_-(\delta_0), \hat{\theta}_+(\delta_0)]$  (red plus) as a function of  $N$ . (c) Posterior pdf  $f_{\Theta(\delta_0)|C(\delta_0)}$  for  $N = 5000$ . (d) Optimal deadband width  $\delta_{opt}$  as a function of  $N$  in Example 1.

where  $e(t)$  is a Gaussian white noise with zero mean and standard deviation 4. Fig. 4(a) shows some samples of  $x(t)$ , together with a high-alarm threshold  $x_{th} = 1$ . By assuming that  $x(t)$  is in normal condition, many false alarms occur in the alarm variable  $x_a(t)$ , as shown in Fig. 4(b). An alarm deadband is designed to remove 95% of false alarms, that is, the number of false alarms in  $x_a(t)$ ;  $d$ ) from the alarm deadband should be about 5% of false alarms in  $x_a(t)$ .

The proposed method is applied to  $\{x(t)\}_{t=1}^N$  for different values of  $N$ . The upper bound of deadband widths in (11) is calculated as  $\delta_{max} = 2.633$ . All samples of the maximum amplitude deviation for  $N = 5000$  are given as  $\{\delta(k)\}_{k=1}^{K=338}$  in Fig. 5(a). As  $N$  and  $K$  increase, the confidence interval  $[\hat{\theta}_-(\delta_0), \hat{\theta}_+(\delta_0)]$  in Fig. 5(b) becomes narrower, so that the estimated cumulative probability  $\hat{\theta}(\delta_0)$  gets more reliable. As shown in Fig. 5(d), the optimal deadband width  $\delta_{opt} = \delta_0 = 1.685$  is found to be the one such that  $\hat{\theta}(\delta_0) = 0.05$  is closest to  $\eta_0 = 0.05$ . Fig. 5(c) shows the corresponding posterior pdf  $f_{\Theta(\delta_0)|C(\delta_0)}$ . By taking the confidence level 95%, the confidence interval  $[\hat{\theta}_-(\delta_0), \hat{\theta}_+(\delta_0)]$  is  $[0.023, 0.071]$ , and

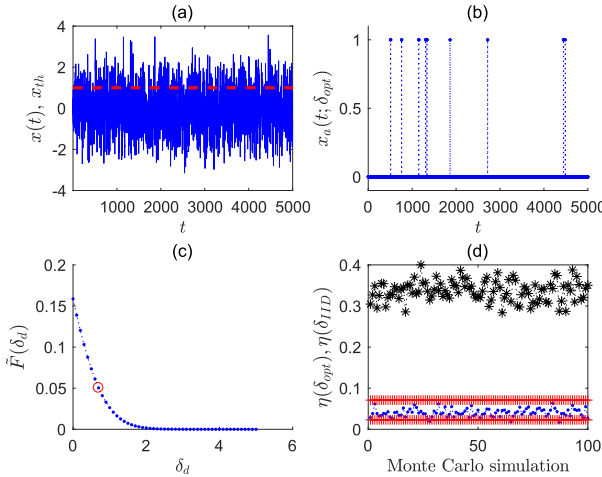


Fig. 6. (a)  $x(t)$  (blue solid) and a high-alarm threshold  $x_{th}$  (red dash). (b)  $x_a(t; \delta_{opt})$ . (c)  $\tilde{F}(\delta_d)$  in (26). (d)  $\eta(\delta_{opt})$  (blue dot) with the confidence interval [0.023, 0.071] (red plus) and  $\eta(\delta_{IID})$  (black star) in Example 1.

the ratio  $r(\hat{\theta}(\delta_0))$  in (23) is equal to 1.8519, being larger than  $\beta = 1$ . Hence, the estimated probability  $\hat{\theta}(\delta_0) = 0.05$  is reliable, so that  $\delta_{opt} = 1.685$  is trustworthy. In other words, the ratio  $\eta(\delta_{opt})$  is expected to be 0.05 in the confidence interval [0.023, 0.071] with a confidence level 95%.

As a validation, 100 Monte Carlo simulations are performed for  $N = 5000$ . Fig. 6(a) and (b) presents samples of  $x(t)$  and  $x_a(t; \delta_{opt})$  in one typical simulation. By using  $\delta_{opt} = 1.685$ ,  $\eta(\delta_{opt})$ 's in 100 simulations are given as blue dots in Fig. 6(d). For 97 simulations,  $\eta(\delta_{opt})$ 's are inside the confidence interval [0.023, 0.071], which is consistent with expectations.

For comparison, existing design methods are applied, based on the process variable  $x(t)$ . If  $x(t)$  is IID, then  $x(t)$  is equivalent to a random variable  $x$  with the pdf  $f(x)$ . If an FAR is defined as the percentage of samples in  $\{x_a(t; \delta_d)\}_{t=1}^N$  in the alarm state when  $\{x(t)\}_{t=1}^N$  is in normal condition, that is,

$$\tilde{F}(x_a(t; \delta_d)) = \frac{\sum_{t=1}^N x_a(t; \delta_d)}{N} \quad (25)$$

then it is ready to derive that the FAR for an alarm deadband in (2) has a theoretical expression

$$\tilde{F}(\delta_d) = \frac{\int_{x_{th}+\delta_d}^{+\infty} f(x) dx}{\int_{x_{th}+\delta_d}^{+\infty} f(x) dx + \int_{-\infty}^{x_{th}} f(x) dx}. \quad (26)$$

Analogous to (10), an optimal deadband width can be designed as

$$\delta_{IID} = \min\{\delta_{max}, \arg \min_{\delta_d} |\tilde{F}(\delta_d) - \tilde{F}_0|\} \quad (27)$$

where  $\tilde{F}_0$  is a user-selected desired FAR value. Fig. 6(c) presents the FAR function  $\tilde{F}(\delta_d)$  in (26), from which  $\delta_{IID} = 0.7$  is obtained from (27). For the 100 Monte Carlo simulations, too many false alarms are left by using  $\delta_{IID} = 0.7$ , and  $\eta(\delta_{IID})$ 's in Fig. 6(d) are about 0.35, much than the desired value 0.05. Since the process variable  $x(t)$  is not IID,  $\tilde{F}(\delta_d)$  in (26) are invalid. Hence, the unsatisfactory performance of  $\delta_{IID}$  is essentially due to the invalid assumption that  $x(t)$  is IID.

TABLE I  
SENSITIVITY ANALYSIS OF  $\beta$  FOR EXAMPLE 1

$\beta$	$\delta_{opt}$	$r(\hat{\theta}(\delta_{opt}))$
0.7	1.9870	0.7574
0.9	1.7893	0.9506
1	1.6699	1.8519
2	1.6614	2.1739
3	1.6298	3.5714

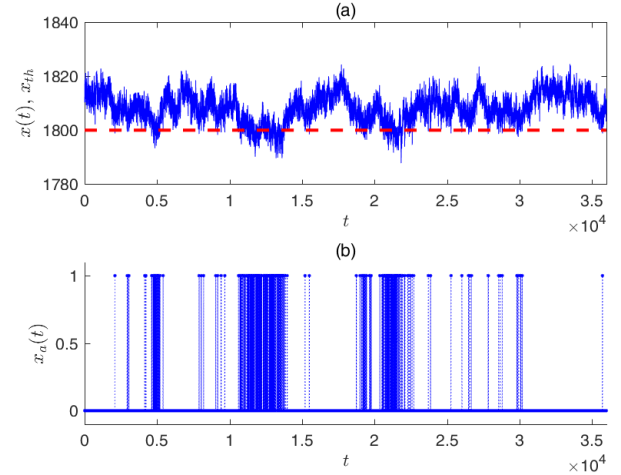


Fig. 7. (a)  $x(t)$  (blue solid) and a low-alarm threshold  $x_{th}$  (red dash). (b)  $x_a(t)$  in Example 2.

A sensitivity analysis of  $\beta$  in (23) is performed here. Fig. 5(b) marks the positions of  $\hat{\theta}(\delta_0)$ 's for five values of  $\beta$ , and Table I lists the corresponding values of  $\delta_{opt}$ . As shown in Fig. 5(b) and Table I,  $\hat{\theta}(\delta_0)$  and its confidence interval  $[\hat{\theta}_-(\delta_0), \hat{\theta}_+(\delta_0)]$  begin to change slowly at about  $\beta = 1$ , and the differences among  $\delta_{opt}$ 's for  $\beta = 1, 2, 3$  are quite small. Hence,  $\beta = 1$  is chosen as the default value, saying that  $\hat{\theta}(\delta_0)$  should be equal to or larger than its estimation uncertainty  $\max(\hat{\theta}(\delta_0) - \hat{\theta}_-(\delta_0), \hat{\theta}_+(\delta_0) - \hat{\theta}(\delta_0))$ .

*Example 2:* The proposed method has been successfully applied to more than 100 process variables in a 300-MW coal-fired thermal power plant. This example presents the results for a typical process variable  $x(t)$  in the unit  $\text{Nm}^3/\text{h}$  with tagname X71NAO084 as the inlet air flow of an ammonia-air mixer. It is a common flow rate variable, being configured with a low-alarm threshold  $x_{th} = 1800 \text{ Nm}^3/\text{h}$ . The number of false alarms in this variable is the largest among all process variables being investigated. The optimal deadband width is designed in an offline manner based on historical samples under normal conditions. Then, it is taken as the parameter of an alarm deadband function (such as the HLALM function in Fig. 1) in distributed control systems to reduce false alarms in an online manner.

Fig. 7(a) shows 10-h samples of  $x(t)$  with a sample period 1 s. Industrial plant operators confirm that  $x(t)$  in the 10 h are indeed in the normal condition, so that all occurred alarms in Fig. 7(b) are false ones. It is required to design an alarm deadband for removing 95% of false alarms in upcoming time periods.

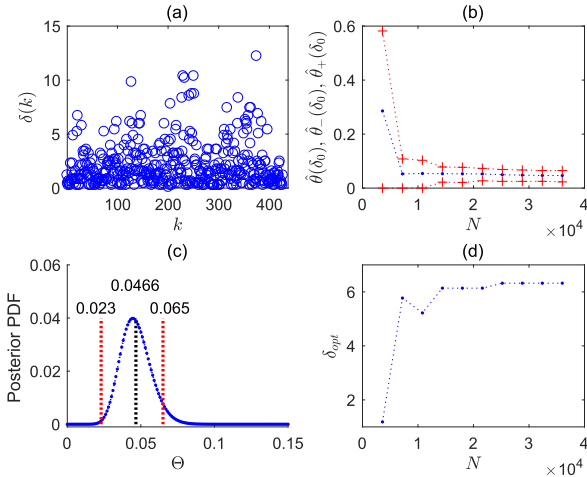


Fig. 8. (a)  $\{\delta(k)\}_{k=1}^{K=427}$ . (b)  $\hat{\theta}(\delta_0)$  (blue dot) and its confidence interval  $[\hat{\theta}_-(\delta_0), \hat{\theta}_+(\delta_0)]$  (red plus) as a function of  $N$ . (c)  $f_{\Theta(\delta_0)|C(\delta_0)}$  based on all maximum amplitude deviations. (d)  $\delta_{opt}$  as a function of  $N$  in Example 2.

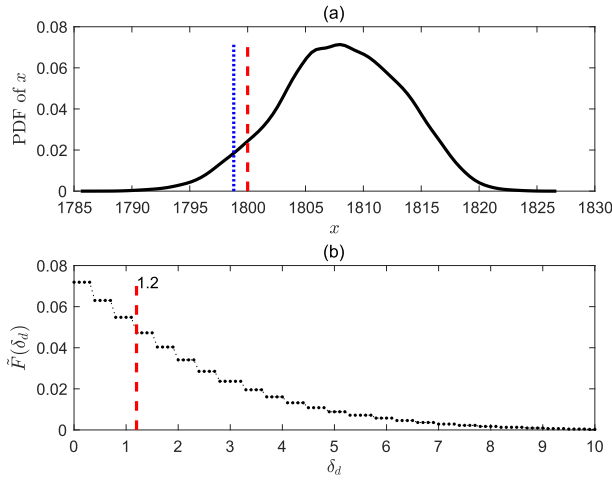


Fig. 9. (a) Estimated pdf of  $x(t)$  (black dot), a low-alarm threshold  $x_{th}$  (red dash) and  $x_{th} - \delta_{IID}$  (blue solid). (b)  $\tilde{F}(\delta_d)$  in (26) (black dot) and  $\delta_{IID}$  (red dash) in Example 2.

The proposed method is applied first. Fig. 8(a) presents all samples  $\{\delta(k)\}_{k=1}^{K=427}$  of the maximum amplitude deviation in the ten hours. By increasing  $N$  with a step of 3600 samples from the first hour till the tenth, the proposed method yields the estimated cumulative probability  $\hat{\theta}(\delta_0)$  with its confidence interval  $[\hat{\theta}_-(\delta_0), \hat{\theta}_+(\delta_0)]$  as a function of  $N$  in Fig. 8(b), as well as the corresponding optimal deadband width  $\delta_{opt}$  as a function of  $N$  in Fig. 8(d). As  $N$  gets larger, the confidence interval becomes narrower. For the entire samples  $\{\delta(k)\}_{k=1}^{K=427}$  in the 10 h,  $\delta_0 = 6.3223$  is the one such that  $\hat{\theta}(\delta_0) = 0.04662$  is the closest to  $\eta_0 = 0.05$ . The corresponding posterior pdf  $f_{\Theta(\delta_0)|C(\delta_0)}$  is given in Fig. 8(c). The confidence interval  $[\hat{\theta}_-(\delta_0), \hat{\theta}_+(\delta_0)]$  is  $[0.023, 0.065]$  for the confidence level 95%, and the ratio  $r(\hat{\theta}(\delta_0)) = 1.9737$  is larger than the threshold  $\beta = 1$ . Hence,  $\hat{\theta}(\delta_0)$  is reliable so that  $\delta_{opt} = 6.3223$  is trustworthy. Note that the upper bound  $\delta_{max}$  in (11) is calculated as 6.577.

The existing method is applied for comparison. For the 10-h samples of  $x(t)$ , the pdf of  $x$  is estimated via a standard kernel

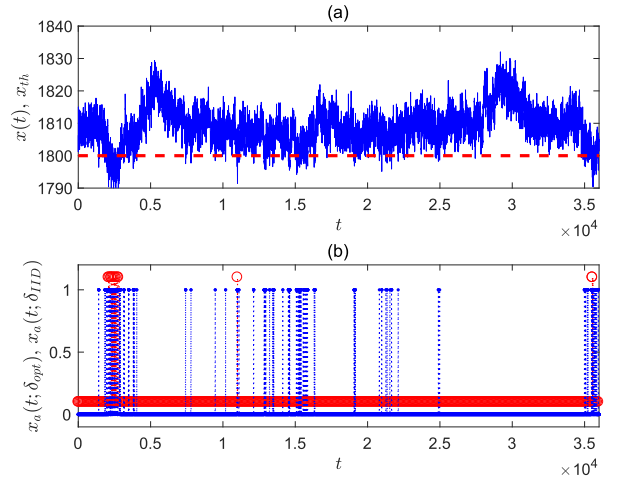


Fig. 10. (a) 8-h samples of  $x(t)$  (blue solid) and a low-alarm threshold  $x_{th}$  (red dash). (b)  $x_a(t; \delta_{opt})$  (red circle, shifted upward for 0.1) and  $x_a(t; \delta_{IID})$  (blue dot) in Example 2.

pdf estimation method, as shown in Fig. 9(a). Based on the estimated pdf of  $x$ , the FAR function  $F(\delta_d)$  is calculated as given in Fig. 9(b), leading to  $\delta_{IID} = 1.2$ .

The two deadband widths  $\delta_{opt} = 6.322$  and  $\delta_{IID} = 1.2$  are applied to a new set of 8-h samples of  $x(t)$ . Fig. 10 depicts the samples of  $x(t)$  as well as the alarm variables  $x(t; \delta_{opt})$  and  $x(t; \delta_{IID})$ . The unremoved false alarm ratio  $\eta(\delta_{opt})$  is equal to 0.0483, which is close to the desired value 0.05. By contrast,  $\eta(\delta_{IID}) = 0.4897$  is much larger than the design specification 0.05. Only half of the false alarms in  $x_a(t)$  are removed by using  $\delta_{IID}$ . The failure of  $\delta_{IID} = 1.2$  is due to the invalid assumption that  $x(t)$  is IID. As shown in Fig. 7(a) and Fig. 10(a),  $x(t)$  is clearly not IID.

## V. CONCLUSION

This brief proposed a new method to design alarm deadbands for removing a desired percentage of false alarms. First, maximum amplitude deviations were calculated from historical samples of process variables in the normal condition. Second, an optimal value of the deadband width was chosen as the maximum amplitude deviation achieving a desired cumulative probability. The Bayesian estimation approach was exploited to tell whether the estimated cumulative probability was reliable. Unlike existing methods, the proposed one had no discriminations to IID and non-IID process variables.

One future work is to deploy the proposed method for multivariate situations. Let us take multivariate statistical methods [25] as examples. These methods usually compare some statistics, such as  $T^2$  statistic in principal component analysis, to their control limits to monitor abnormal conditions. By treating such a statistic as a process variable, the proposed method is ready to be applied to reduce false alarms being associated with the statistic.

## REFERENCES

- [1] ISA-18.2: *Management of Alarm Systems for the Process Industries*, Int. Soc. Automat., Research Triangle Park, NC, USA, 2009.
- [2] EEMUA-191: *Alarm Systems—A Guide to Design, Management and Procurement*, Eng. Equip. Mater. Users Assoc., Kenilworth, U.K., 2013.

- [3] M. L. Bransby and J. Jenkinson, *The Management of Alarm Systems*. Bootle, U.K.: Health and Safety Executive, 1998.
- [4] D. Rothenberg, *Alarm Management for Process Control*. New York, NY, USA: Momentum Press, 2009.
- [5] B. Hollifield and E. Habibi, *The Alarm Management Handbook*, 2nd ed. Research Triangle Park, NC, USA: PAS, 2010.
- [6] J. Wang, Y. Zhao, and Z. Bi, "Criteria and algorithms for online and offline detections of industrial alarm floods," *IEEE Trans. Control Syst. Technol.*, vol. 26, no. 5, pp. 1722–1731, Sep. 2018.
- [7] P. Goel, A. Datta, and M. S. Mannan, "Industrial alarm systems: Challenges and opportunities," *J. Loss Prevention Process Ind.*, vol. 50, pp. 23–36, Nov. 2017.
- [8] J. Xu, J. Wang, I. Izadi, and T. Chen, "Performance assessment and design for univariate alarm systems based on FAR, MAR, and AAD," *IEEE Trans. Autom. Sci. Eng.*, vol. 9, no. 2, pp. 296–307, Apr. 2012.
- [9] A. Tulsyan, F. Alrowaie, and B. Gopaluni, "Design and assessment of delay timer alarm systems for nonlinear chemical processes," *AICHE J.*, vol. 64, no. 1, pp. 77–90, 2018.
- [10] R. Kaced, A. Kouadri, and K. Baiche, "Designing alarm system using modified generalized delay-timer," *J. Loss Prevention Process Industries*, vol. 61, pp. 40–48, Sep. 2019.
- [11] A. J. Hugo, "Estimation of alarm deadbands," in *Proc. 7th IFAC Symp. Fault Detection, Supervision Saf. Tech. Processes*, Barcelona, Spain, Jun. 2009, pp. 663–667.
- [12] I. Izadi, S. L. Shah, D. S. Shook, S. R. Kondaveeti, and T. Chen, "A framework for optimal design of alarm systems," in *Proc. 7th IFAC Symp. Fault Detection, Supervision Saf. Tech. Processes*, Barcelona, Spain, Jun. 2009, pp. 651–656.
- [13] N. A. Adnan, I. Izadi, and T. Chen, "On expected detection delays for alarm systems with deadbands and delay-timers," *J. Process Control*, vol. 21, no. 9, pp. 1318–1331, 2011.
- [14] E. Naghoshi, I. Izadi, and T. Chen, "Estimation of alarm chattering," *J. Process Control*, vol. 21, no. 9, pp. 1243–1249, Oct. 2011.
- [15] M. S. Afzal, T. Chen, A. Bandekhoda, and I. Izadi, "Analysis and design of time-deadbands for univariate alarm systems," *Control Eng. Pract.*, vol. 71, pp. 96–107, Feb. 2018.
- [16] H. Huawei, W. Chunli, S. Ning, and J. Weiwei, "Design of intelligent alarm system for petrochemical process," in *Proc. Chin. Control Decis. Conf. (CCDC)*, Shenyang, China, Jun. 2018, pp. 5059–5064.
- [17] A. Tulsyan and R. B. Gopaluni, "Univariate model-based deadband alarm design for nonlinear processes," *Ind. Eng. Chem. Res.*, vol. 58, no. 26, pp. 11295–11302, Jul. 2019.
- [18] Z. Wang, X. Bai, J. Wang, and Z. Yang, "Indexing and designing deadbands for industrial alarm signals," *IEEE Trans. Ind. Electron.*, vol. 66, no. 10, pp. 8093–8103, Oct. 2019.
- [19] K. Aslansefat, M. Bahar Gogani, S. Kabir, M. A. Shoorehdeli, and M. Yari, "Performance evaluation and design for variable threshold alarm systems through semi-Markov process," *ISA Trans.*, vol. 97, pp. 282–295, Feb. 2020.
- [20] Y. T. P. Nunes, R. S. de Abreu, G. Leitao, and L. A. Guedes, "An optimization-based method to define dead-band values of industrial alarms," in *Proc. CBA-Congresso Brasileiro de Automatica*, Fortaleza, Brazil, Oct. 2022, P. 4899.
- [21] M. Asaadi, I. Izadi, A. Hassanzadeh, and F. Yang, "Assessment of alarm systems for mixture processes and intermittent faults," *J. Process Control*, vol. 114, pp. 120–130, Jun. 2022.
- [22] J. L. Devore, *Probability and Statistics for Engineering and The Sciences*, 5th ed. London, U.K.: Thomson Learning, 2004, pp. 257–258.
- [23] A. E. Doan, "Type I and type II error," *Encyclopedia Social Meas.*, vol. 3, pp. 883–888, May 2005.
- [24] R. E. Walpole, R. H. Myers, S. L. Myers, and K. Ye, *Probability and Statistics for Engineers and Scientists*, 9th ed. Upper Saddle River, NJ, USA: Prentice-Hall, 2011.
- [25] R. Kaced, A. Kouadri, K. Baiche, and A. Bensmail, "Multivariate nuisance alarm management in chemical processes," *J. Loss Prevention Process Industries*, vol. 72, Sep. 2021, Art. no. 104548.